

A Study of Slip Position on Improving the Hydrodynamic Lubrication Performance of Single-Textured Bearing using a Mass Conserving Numerical Approach

M. Tauvqirrahman^{#1}, W. K. Ajie[#], E. Yohana[#], M. Muchammad^{*2}, J. Jamari[#]

[#]Laboratory for Engineering Design and Tribology,
Department of Mechanical Engineering, University of Diponegoro
Jl. Prof. Soedharto, Tembalang, Semarang, Indonesia, Phone: 024-7460059

¹mohammad.tauvqirrahman@ft.undip.ac.id

^{*}Laboratory for Surface Technology and Tribology,
Faculty of Engineering Technology, University of Twente
Drienerloolaan 5, Postbus 217, 7500 AE, Enschede, The Netherlands

²m_mad5373@yahoo.com

Abstract—More and more studies have demonstrated theoretically and experimentally that the application of boundary slip as well as surface texturing can be beneficial in lubricated couples (mechanical seals, cylinder-liner contacts, and hydrodynamic bearings). However, most of studies did not consider the cavitation characteristic appropriately. This paper investigates the optimal hydrodynamic performance of single-textured bearing under cavitation effect using a mass-conserving numerical approach, aiming to help designers obtain appropriate design parameters. A modified Reynolds equation including slip is developed with consideration of the cavitation mechanism based on JFO theory. It is confirmed that adding slip at the leading edge of the single-textured contact is considered more efficient than extending the slip to the textured region with respect to the load support and friction force. The results also indicate that the slip inlet length as well as the pocket length has a huge impact on performance characteristics.

Keyword- cavitation, hydrodynamic lubrication, slip, texture

I. INTRODUCTION

Surface texturing has been shown to improve the load support and reduce friction in various components such as mechanical seals [1-4], cylinder-liner contacts [5-7] and hydrodynamic parallel slider bearings [8-13]. Although some findings regarding texturing parameters such as texture depth, width, number of dimples, location of the dimples, and texture shapes for typical bearing applications under hydrodynamic situations have been established, obtaining optimal texturing parameters is still very challenging. In addition to texturing, in order to tackle lubrication problem, another potential attractive technique is by introducing a surface with boundary slip. Motivation is based on the idea of achieving the friction reduction through boundary slip in hydrodynamically lubricated contacts. The most promising technique to yield the boundary slip originates from investigations by coating the contacting surface in a controlled way by hydrophobic layer. Control of boundary slip will allow a degree of verification over the hydrodynamic performance in confined systems and is important in lubricated bearing. Recently, due to the progress in micrometer measurement technology, promising research on the improvement of reliability for hydrodynamic bearing is proceeding with respect to the use of the engineered slip. A number of excellent works have demonstrated that the boundary slip on hydrophobic surface results in a significant friction reduction in lubricated sliding contacts [14, 15].

Several studies have proven that combining texturing with boundary slip can be beneficial with respect to the hydrodynamic performance. More and more attention is paid to textured bearings with boundary slip instead of conventional textured bearings (without boundary slip). It is worth mentioning the early work of Salant and Fortier [16], who explored the combined effect of the slip and the recess in bearing. The results illustrated that recess and slip in bearing yield higher load support and lower friction compared to conventional bearing (without slip). Rao et al. [17, 18] concluded analytically that the partially textured slip parallel lubricated contact either in single-texture or multiple textures mode leads to a substantial improvement in the performance characteristics in comparison with identical non-textured/no-slip bearing. Tauvqirrahman et al. [19] investigated the possibility of enhancing the hydrodynamic performance characteristic (high load support combined with low friction) of textured contact by applying the boundary slip. They concluded that compared with the solely textured contact, the predicted improvement in the load support is around 150–300%, while the reduction in the coefficient of friction is about 70–80%. One conclusion that emerges from these studies is that

textured bearing with slip has an advantage over conventional textured bearing. It has come to a consensus that the load support improvement as well as the friction reduction can be obtained by introducing the boundary slip only on part of the textured contact. In general, the previous researches have shown that combining the boundary slip and the texturing has a beneficial effect by increasing the load support and decreasing the friction in bearing. Therefore, the potential application of slip-textured bearings is enormous, and includes shipbuilding, robotic devices, chemical industry, etc. However, in the vast majority of research in the field of textured bearing with slip, the Reynolds boundary condition is quite often adopted, but it does not respect mass conservation and cannot interpret the oil film reformation adequately. As discussed by Ausas et al. [20], the high overestimation of the predicted load support of textured contact may occur if non-mass conserving approach of cavitation is used. The same trend is also found in the case of slip surfaces [21]. Also, as explained in recent publication [22], depending on the specific operating conditions the cavitation can be either the source of the positive effect or the negative effect on the overall contact performance. The unique structure of the slip-textured bearing makes its cavitation characteristics different from conventional bearings. Therefore, to get more accurate results a mass conserving implementation of cavitation is important in the field of boundary slip as well as the surface texturing.

Following this new insight on the bases of the mass conserving treatment of cavitation and the modified slip length model, Fatu et al. [23] investigated the influence of boundary slip on load support and power loss in hydrodynamic slip/no-slip surface pattern bearing. The key finding for textured bearing with slip is that that well-chosen complex slip surface pattern can considerably improve the bearing behavior and inappropriate choice can lead to a drastic deterioration of the bearing performance, especially in relation to support. Later, Wang and Lu [21] have taken into account the cavitation effect for two-dimensional sleeve bearing. They compared the obtained results between the mass-conserving treatment of cavitation and the Reynolds boundary condition. It was concluded that the lubrication performance (the liquid hydrodynamic pressure, load support and friction drag) are larger, and the oil film break-down delays considering mass-conserving boundary condition compared with reckoning with Reynolds boundary condition.

In most numerical works that study the influence of boundary slip in lubricated smooth surfaces, for instance in [16, 24-26], it was suggested that for high lubrication performance, the boundary slip should be applied at the leading edge of the contact, which may be comparable with the partial texturing. Therefore, in the following computations, the main single-textured bearing studied is the bearing which has a boundary slip at the inlet region. The analysis will be carried out to investigate the effect of the slip inlet length on the lubrication performance. The next examination is focused on the effect of combining the slip with the texture cell. As explained in [17, 19], it is more favourable to apply slip at the texture cell compared with conventional texture cell. However, the results suggested in [17, 19] prevails for micro-texture (i.e. multiple textures) instead of single texture of the lubricated sliding contact. It is also noted that the non-mass conserving treatment of cavitation was adopted, which may lead to less accurate results.

While considering this scientific context, the main aim of this work is to study the effects induced by boundary slip in single-textured bearing using a more appropriate investigation while ensuring mass flow conservation. The modified lubrication mathematical formulation, which is mainly based on Reynolds theory and Jakobsson-Floberg-Olsson (JFO) theory [27, 28] of separating the fluid film into two regions, is proposed in Eq. (1). In order to achieve this, two main cases are considered regarding with the location of the slip. Firstly, slip is applied at the leading edge of the contact, and secondly, the slip is introduced both at the inlet and at texture cell edges.

II. MATHEMATICAL MODEL AND ITS SOLUTION

In order to investigate the effect of the slip position for lubricated textured contact, computations have been made by comparing two configurations as indicated in Table I. Two overall sketches of the geometry of single-textured bearing with boundary slip are shown in Fig. 1. In the present work, the shape of the texture cell is chosen to be rectangular as this would be relatively easy to accomplish.

TABLE I. Slip-Textured Contact with Two Possible Boundary Conditions

	Inlet region	Textured region
Configuration 1	Slip	No-slip
Configuration 2	Slip	Slip

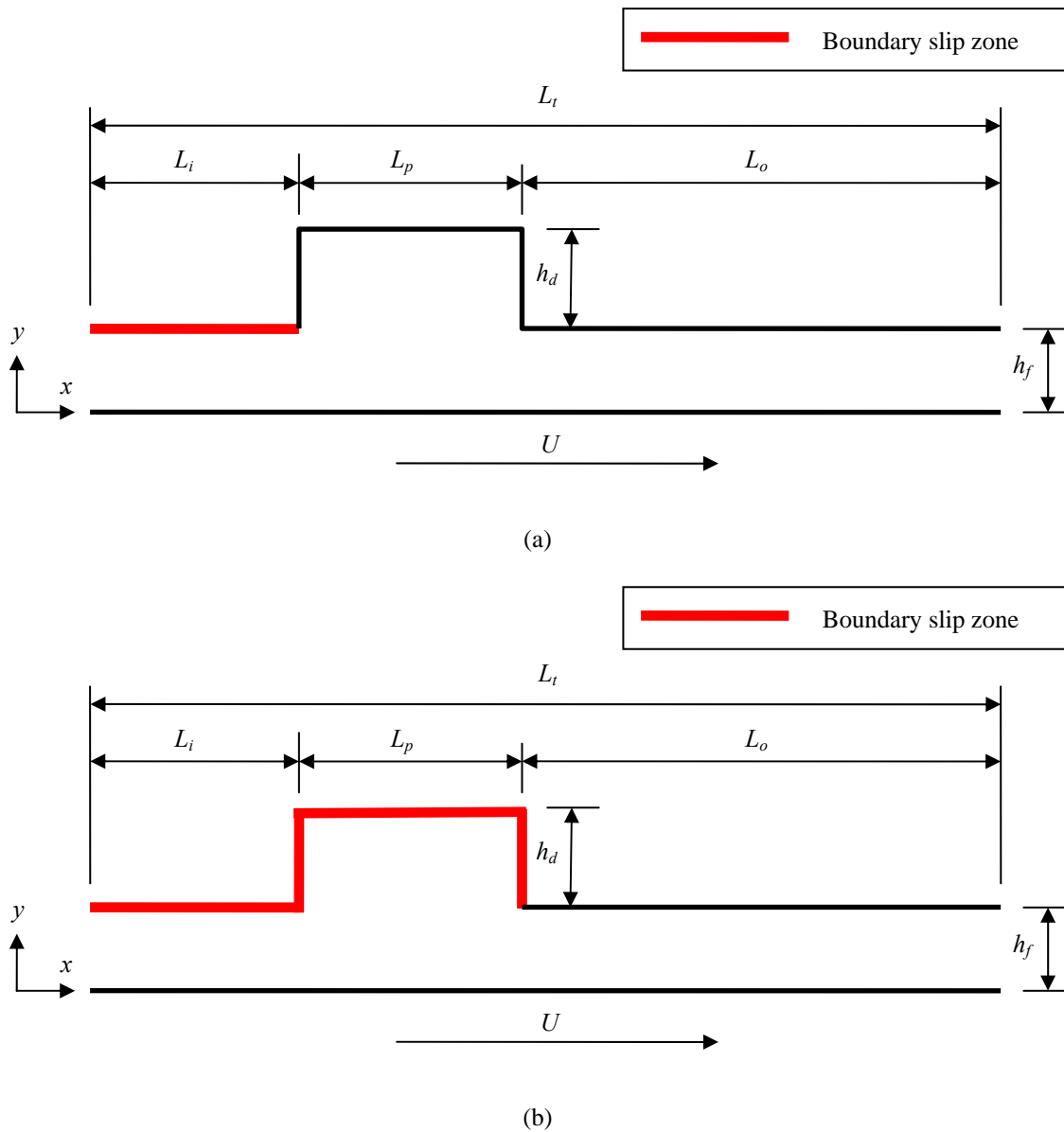


Fig. 1. Two configurations of single-textured bearing with boundary slip: (a) configuration 1, (b) configuration 2

In order to obtain the governing equation of the lubrication problem, it is necessary to define the surface boundary conditions. Let us consider a lubricated contact equivalent to a lower plane moving in the x-direction with surface velocity U , and an upper stationary surface, as shown Fig. 1. On the stationary surface, the boundary slip is applied based on Navier-slip [29]. Such a lubrication system can be described with the modified Reynolds equation as indicated in Eq. (1). Fluid film rupture and reformation in a mass conservative way is modeled using JFO theory. The methodology used to describe the cavitation phenomena is similar to the work of Gherca et al. [30].

$$\left\{ \frac{\partial}{\partial x} \left(\frac{h^3}{12\eta} \frac{\partial D}{\partial x} \frac{h^2 + 4h\alpha\eta}{h(h+\eta\alpha)} \right) \right\} F = \frac{U}{2} \frac{\partial}{\partial x} \left(\frac{h^2 + 2h\alpha\eta}{h + \eta\alpha} \right) - U \frac{\alpha\eta}{h + \alpha\eta} \frac{\partial h}{\partial x} + \frac{h}{2\eta} \frac{h\alpha\eta}{h + \alpha\eta} \left(\frac{\partial D}{\partial x} \frac{\partial h}{\partial x} \right) F \quad (1)$$

$$+ \left\{ \frac{U}{2} \frac{\partial}{\partial x} \left(\frac{D}{h} \frac{h^2 + 2h\alpha\eta}{h + \eta\alpha} \right) - \frac{D}{h} U \frac{\alpha\eta}{h + \eta\alpha} \frac{\partial h}{\partial x} \right\} (1 - F)$$

It should be noted that the modified Reynolds equation developed here (Eq. 1) is derived for over the whole bearing. Thus, the universal function D and so-called index function F are utilized and defined below.

- In lubricated zone:

$$\begin{cases} D = p - p_{cav} \\ F = 1 \end{cases} \quad D \geq 0$$

- In cavitation zone:

$$\begin{cases} D = r - h, \\ F = 0 \end{cases} \quad D < 0$$

where p_{cav} represents the cavitation pressure and $r = (\rho/\rho_o)h$. In this study, for simplification, p_{cav} is assumed constant for simplification reasons. Here, ρ defines the density of lubricant in lubricated zone, while ρ_o defines the density of mixture of oil and gas. For the case where $F = 1$, Eq. (1) reduces into a simpler form of the modified Reynolds equation with slip for incompressible fluids:

$$\begin{aligned} \frac{\partial}{\partial x} \left(\frac{h^3}{12\eta} \frac{\partial(p - p_{cav})}{\partial x} \frac{h^2 + 4h\eta\alpha}{h(h + \eta\alpha)} \right) &= \frac{U}{2} \frac{\partial}{\partial x} \left(\frac{h^2 + 2h\alpha\eta}{h + \eta\alpha} \right) \\ -U \frac{\alpha\eta}{h + \alpha\eta} \frac{\partial h}{\partial x} + \frac{h}{2\eta} \frac{h\alpha\eta}{h + \alpha\eta} \left(\frac{\partial(p - p_{cav})}{\partial x} \frac{\partial h}{\partial x} \right) & \end{aligned} \quad (2)$$

The physical meanings of the symbols in Eq. (1) are as follows: h the film thickness (gap), p the lubrication film hydrodynamic pressure, α the slip coefficient on the stationary surface, U = Sliding velocity and η the lubricant viscosity. All parameters and the range in which they are varied for all cases investigated in the present study are summarized in Table II. In the present work, the slip coefficient is set to 0.05 m²/kg, that is an optimal value for achieving the highest lubrication performance (high load support and low friction) as confirmed by [18, 24].

TABLE II. Main Bearing Characteristics Studied

Total length	L_t	0.02 m
Sliding velocity	U	1 m/s
Dynamic viscosity	η	0.01 Pa s
Land film thickness	h_f	1 μm
Atmospheric pressure	P_{atm}	100 kPa
Cavitation pressure	P_{cav}	0 kPa

In order to solve Eqs. (1)–(3), a numerical method is required. To this end, the finite difference equations obtained by means of the micro-control volume approach [31] was used. The entire computational domain is conditioned as a full hydrodynamic lubrication. By applying the discretization scheme, the computational domain is divided into a number of control volumes. The mesh number for all the cases obtained from a mesh refinement study has ranges from 4,000 to 6,000 nodes depend on the texture geometry.

In the present work, the bearing is operating under steady state assumption. The load support is obtained by integrating the calculated hydrodynamic pressure field along the contact surface. The friction force is predicted by integrating the surface shear stress over the surface area.

III. RESULTS AND DISCUSSIONS

A. The Effect of slip inlet length

To investigate the effect of the position of boundary slip on the lubrication performance of single-textured surfaces with respect to the enhancement of the load support and the friction force, various parameters are set up. The length of the inlet region L_i in which the slip is located, is varied over a large range of value. In the present work, the dimensionless inlet length L_i/L_t is varied from 0.02 to 0.70.

Figure 2 presents the effect of dimensionless inlet length L_i/L_t and the dimensionless pocket depth H_d on the load support W (Fig. 2a) and the friction force F (Fig. 2b). Two observations can be made based on Fig. 2. At first, the load support increases and then decreases rapidly with the increase in the length of the inlet region. This trend prevails for all configurations considered here both for low H_d and high H_d . It is easy to observe that the optimum dimensionless inlet length L_i/L_t takes values in a narrow interval (0.45 – 0.50) depend on the pocket depth. For example, for configuration 1 (the contact with slip applied at the leading edge of the contact but with no-slip in the pocket region) with pocket depth H_d of 0.25, the inlet length is most effective when $L_i/L_t = 0.45$. However, when the pocket depth H_d for same configuration is increased by a factor 3 (i.e. $H_d = 7.5$), the optimal inlet length occurs a slight shift, i.e. $L_i/L_t = 0.50$. It means that for improving the load support significantly, the pocket depth does not need to be sufficiently increased. One can remark that in the case of

combined slip-textured bearing (configuration 2), the predicted load support is 3-30% lower than configuration 1, especially when L_i/L_t is varied between for 0 and 0.50 both for low and high H_d . For example, the textured pocket (without slip in the pocket) at optimal inlet length of 0.45 produces the load support which is just 3% lower than the textured pocket (with slip in the pocket) at optimal inlet length of 0.50 for case of same H_d . It indicates that adding the slip to the pocket does not appear effective to generate more hydrodynamic load support.

Secondly, concerning the effect of the pocket depth, as can be seen in Fig. 2 (a), the textured bearing with low H_d is preferred over that with high H_d . This result prevails for all configurations. For the case in which slip applied only at the leading edge of the contact (configuration 1), the computation of single-textured bearing with $H_d = 2.5$ predicts up to 50% improvement for low L_i/L_t . In the case of textured bearing with H_d of 7.5, the configuration 1 (i.e. slip applied on the inlet region) is not better than the configuration 2 (i.e. slip exists both on the inlet area and the pocket area). It can be said that the presence of boundary slip at the inlet region of the contact have a more significant role compared to the slip presence on the textured region. Another interesting result is that when the optimal inlet length is used in the textured bearing, the discrepancies in load support prediction for each configuration are very small (no more than 3%). On the other words, the calculations using small range of the optimal inlet length, ($L_i/L_t = 0.45 - 0.50$ in this case) yield same results. It means that varying the pocket depth does not help in improving the load support while the slip has been located at the leading edge of the contact.

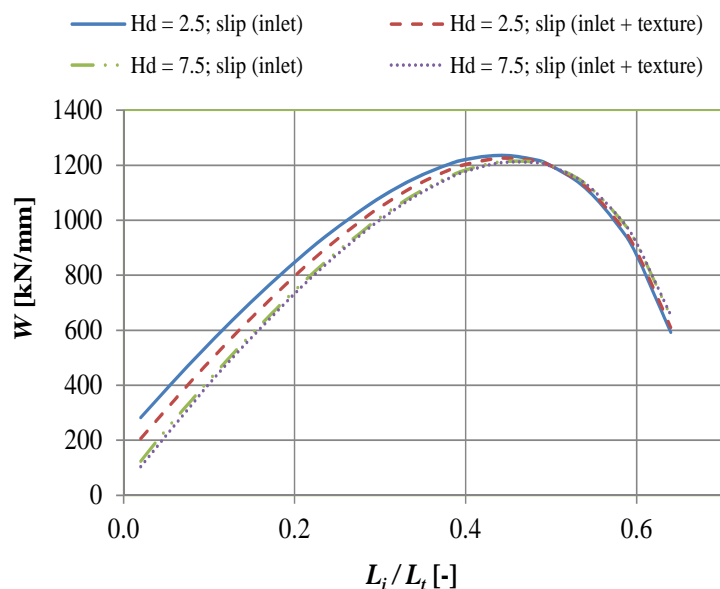


Fig 2. The effect of dimensionless inlet length L_i/L_t on the load support W . The profiles are calculated for dimensionless texture length $L_p/L_t = 0.30$

In Fig. 3, the friction force F of the textured bearing with two slip positions versus the inlet length is presented. It can be observed that increasing the dimensionless inlet length will reduce the friction force. This trend prevails for all configurations considered here. In the case in which the slip is only located at the inlet region, the textured bearing with larger pocket depth produces lower friction force. For a small and large inlet length studied here ($L_i/L_t = 0.02$ and 0.60 in this case), the computation of the textured surface with $H_d = 7.5$ predicts a 11% and 12% enhancement, respectively, compared with the textured surface with $H_d = 2.5$. It is worth noting that when the slip position is extended to the textured region (i.e. configuration 2), the improvement of the friction force by varying the pocket depth has the same result (i.e. around 12%). If the comparison is made for the same pocket depth, adding the slip at the textured region yields a slight 2% and 0.2% improvement, respectively for $H_d = 2.5$ and $H_d = 7.5$. It indicates that locating the boundary slip at the textured region does not have a beneficial effect very much in terms of friction force. This is interesting because this result is consistent with what described in the previous section in terms of load support. However, different with the load support analysis, as can be seen in Fig. 3 that the larger the inlet length, the smaller the friction force. When the inlet length is set to maximum value, the reduction in the friction force is up to 50% for all cases. If the prediction of the friction force is evaluated at the optimal inlet length for the load support ($L_i/L_t = 0.50$), the decrease in F predicted for two configurations with different H_d is high, that is, 32% lower compared to that for the smallest inlet length (i.e. $L_i/L_t = 0.020$).

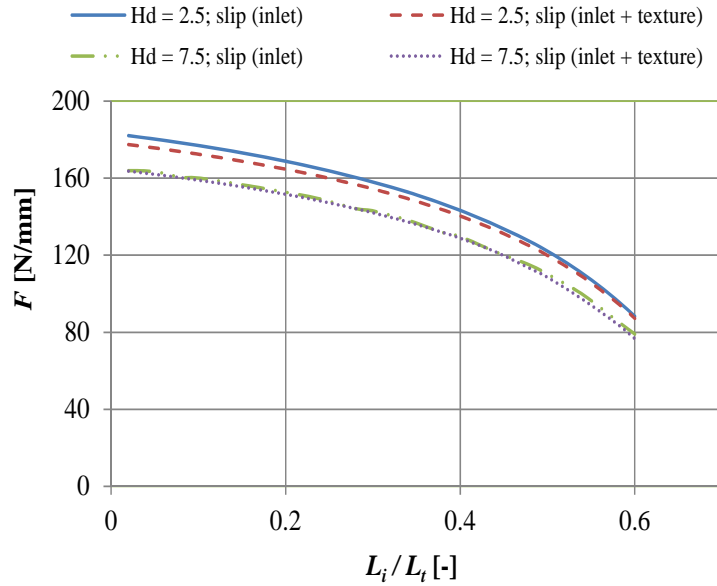


Fig. 3. The effect of dimensionless inlet length L_i / L_t on the friction force F . The profiles are calculated for dimensionless texture length $L_p / L_t = 0.30$.

B. Effect of Texture Cell Length

The effect of dimensionless texture cell length L_p / L_t on the load support W varying the texture depth for two configurations is shown in Fig. 4. Figure 4 reveals that the load support increases and then decreases rapidly with the increase in texture cell length. The existence of optimum texture length that maximizes the load support is noted. Small deviations from the optimum considerably reduce the load support. Based on optimization calculation, the single-textured surface with a textured length which covers 0.55 times the length of the contact ($L_p / L_t = 0.55$) for all configurations is observed. For condition of which the low texture depth is used (i.e. $H_d = 2.5$), the boundary slip is positioned at the inlet region while no-slip presents at the textured region, and the optimal length of textured region (i.e. $L_p / L_t = 0.55$), the highest load support for such bearing is highlighted. When slip is engineered to occur at the texture cell for case of $H_d = 2.5$, the hydrodynamic load support response goes down 7% lower compared to that of texture cell without slip. For case of $H_d = 7.5$, the maximum difference in the load support prediction between two configuration studied here is relatively small, i.e. around 2%. Again, as a concluding remark, it can be said that positioning the boundary slip only at the leading edge of the contact is more effective than extending the slip position up to textured region.

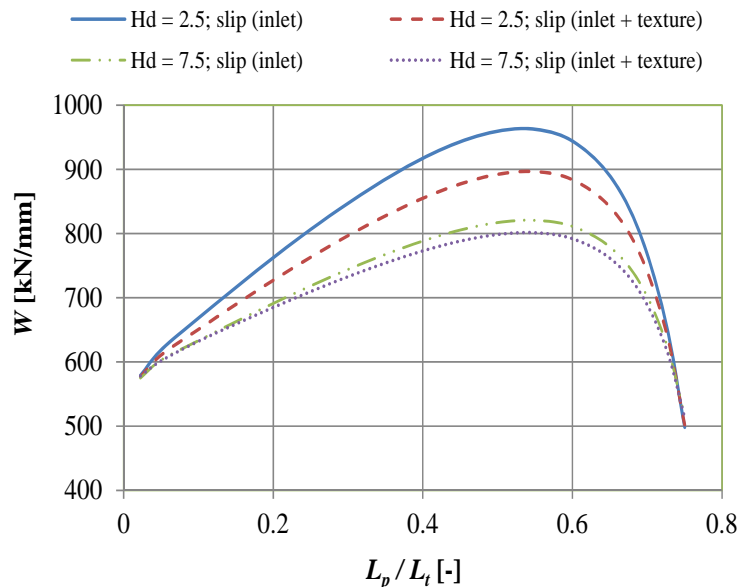


Fig. 4. The effect of dimensionless texture cell length L_p / L_t on the load support W . The profiles are calculated for the inlet length $L_i = 0.004$ m (or $L_i / L_t = 0.20$)

Figure 5 presents the effect of the dimensionless texture cell length L_p/L_t on the friction force F . It can be seen that extending the length of the texture cell (textured region) will reduce the friction force. One can remark that for case of $H_d = 7.5$, configuration 1 (i.e. slip at the inlet) and configuration 2 (i.e. slip at the inlet and textured region) yields the same predictions, especially for low texture cell length. With respect to the extension of the texture cell length, when the maximum length of textured region is chosen (i.e. $L_p/L_t = 0.5$), the friction force can be reduced by 17% (at $H_d = 2.5$) and 33% (at $H_d = 7.5$) for configuration 1 and by 21% (at $H_d = 2.5$) and 36% (at $H_d = 7.5$) for configuration 2, respectively, lower than the single-textured bearing with the minimum length of textured region (i.e. $L_p/L_t = 0.0225$), .

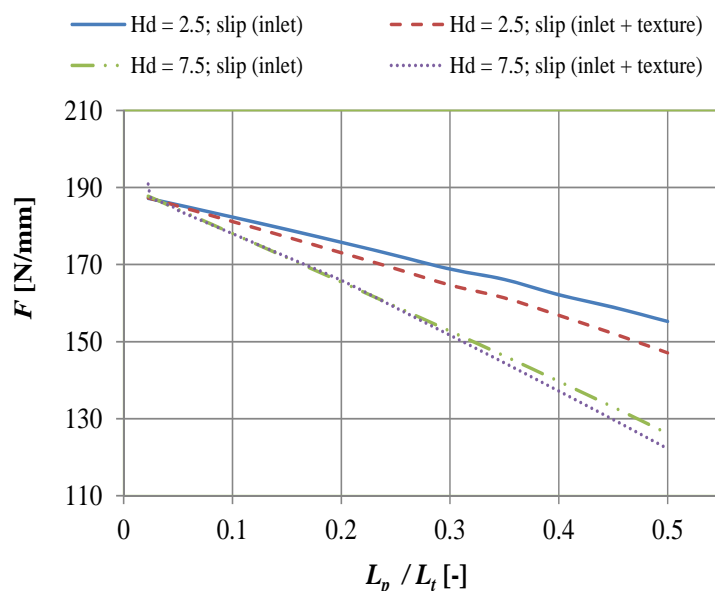


Fig. 5. The effect of dimensionless texture cell length L_p/L_t on the friction force F . The profiles are calculated for the inlet length $L_t = 0.004$ m (or $L_t/L_t = 0.20$)

C. Effect of Texture Depth

Figure 6 compares the load support of configuration 1 and configuration 2 over a wide range of pocket depth. Two observations can be made based on Fig. 6. At first, it can be seen that in the case of configuration 2 (i.e. slip is applied at the leading edge of the contact as well as at the textured region), the lower the texture depth of lubricated sliding contact, the higher the load support. The most possible explanation is that when the pocket texture is very low ($H_d = 0.03$ in this case), the cavitation contribution in the texture to the performance of the load support can be minimized, and therefore the contact behaviour is slightly similar to the smooth surface with boundary slip partly applied at the contact. This is to say that this result matches well with the literature [16, 24-26]. As discussed in previously published works [16, 24-26], such contact leads to the improvement in the load support. Based on the physical point of view, the volume flow induced by slip velocities at the leading edge of the contact is larger than at the outlet, so that the pressure can be produced in order to keep a contact volume flow. As can be seen in Fig. 6, for configuration 2, increasing the texture depth will decrease the load support significantly. A more fundamental indication of this trend is the fact that the slip effect can be vanished by the presence of the texture having high H_d . However, after H_d reaches 6 and above, the load support is not influenced with the further increase in the value for the dimensionless pocket depth.

Secondly, in the case of configuration 1 in which slip is applied at the inlet entrance, one can remark that the optimum value for H_d is placed on $H_d = 0.80$ and that load support is sensitive to the dimensionless pocket depth H_d . Similar to the configuration 2, increasing the pocket depth from 1 to 6 gives a significant effect on the load support. After H_d reaches 6, the pocket depth does not affect the load support considerably. Analyzing Fig. 6, one can see that in order to permit more generation of the load support, the boundary slip is applied at the leading edge of the contact while no boundary slip exists in the pocket area. However, this result is of particular case for high H_d . Because when the pocket depth is low ($H_d < 0.8$ in this case), the slip in the pocket is proven to have more contribution to enhance the load support, and such configuration is comparable with the complex slip surface as discussed earlier. With respect to the friction force, a contradictory result is observed (Fig. 7). Extending the slip up to the pocket region makes the friction prediction lower than the configuration of the pocket without slip especially when H_d reaches 1.5 and above. Other interesting result is that for both configurations, the calculations result in the increase-then-decrease behaviour of the friction force. This is to say that the friction force is sensitive to the pocket depth.

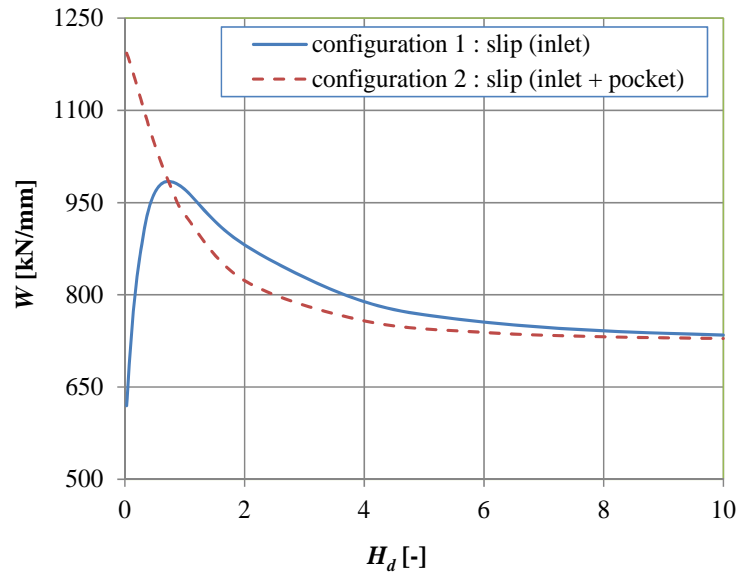


Fig. 6. The effect of dimensionless pocket depth H_d on the load support W . The profiles are calculated for inlet length $L_i = 0.004$ m (or $L_i/L_t = 0.20$) and pocket length $L_p = 0.006$ m (or $L_p/L_t = 0.3$).

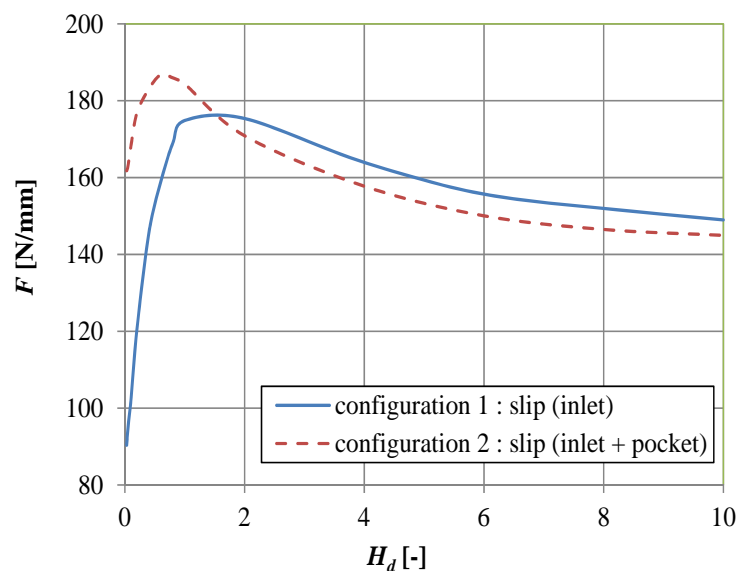


Fig. 7. The effect of dimensionless pocket depth H_d on the friction force F . The profiles are calculated for inlet length $L_i = 0.004$ m (or $L_i/L_t = 0.20$) and pocket length $L_p = 0.006$ m (or $L_p/L_t = 0.3$).

IV. CONCLUSION

The aim of the investigation was to examine whether positioning the boundary slip to the texture cell in full film hydrodynamic lubrication is necessary or not with respect to the hydrodynamic lubrication performance. The modified Reynolds equation with slip combined with a mass conserving treatment of cavitation was derived. The conclusions can be summarized as follows:

- 1 The effect of boundary slip is strongly related to the inlet length instead of the pocket depth. With the purpose of improvement of the load support, slip at the surfaces in textured contact must be located at the inlet region with a slip zone that covers 0.50 of the contact length.
- 2 With respect to the effect of pocket depth, a contradictory result between the load support and friction force analysis is observed. It indicates that the optimal pocket depth should be determined separately depend on the wanted lubrication performance.
- 3 All the results indicate that adding the boundary slip at the textured region would not help either in improving the load support or reducing the friction force.

These findings may be utilized as a guideline for the fabrication of modified sliding textured surfaces in which the boundary slip is introduced in order to double the positive effect of the texturing.

REFERENCES

- [1] X.Q. Yu, S. He and R.L. Cai, "Frictional characteristics of mechanical seals with a laser textured seal face," *J. Mater. Process Technol.*, vol. 129, pp. 463–466, 2002.
- [2] I. Etsion and G. Halperin, "A laser surface textured hydrostatic mechanical seal," *STLE Tribol. Trans.*, vol. 45, pp. 430–434, 2002.
- [3] S. Bai, X. Peng, Y. Li and S. Sheng, "A hydrodynamic laser surface-textured gas mechanical face seal," *Tribol. Lett.*, vol. 38, pp. 187–194, 2010.
- [4] T. Wang, W. Huang, X. Liu, Y. Li and Y. Wang, "Experimental study of two-phase mechanical face seals with laser surface texturing," *Tribol. Int.*, vol. 72, pp. 90–97, 2014.
- [5] G. Ryk, Y. Kligerman and I. Etsion, "Experimental investigation of laser surface texturing for reciprocating automotive components," *Tribol. Trans.*, vol. 45, pp. 444–449, 2002.
- [6] S. Mezghani, I. Demirci, H. Zahouani, and M.E. Mansori, "The effect of groove texture patterns on piston-ring pack friction," *Precis. Eng.*, vol. 36, pp. 210–217, 2012.
- [7] Y. Zhou, H. Zhu, W. Tang, C. Ma and W. Zhang, "Development of the theoretical model for the optimal design of surface texturing on cylinder liner," *Tribol. Int.*, vol. 52, pp. 1–6, 2012.
- [8] I. Etsion, G. Halperin, V. Brizmer and Y. Kligerman, "Experimental investigation of laser surface textured parallel thrust bearing," *Tribol. Lett.*, vol. 17, pp. 295–300, 2004.
- [9] A. Kovalchenko, O. Ajayi, A. Erdemir, G. Fenske and I. Etsion, "The Effect of laser surface texturing on transitions in lubrication regimes during unidirectional sliding contact," *Tribol. Int.*, vol. 38, pp. 219–225, 2005.
- [10] S. Rahmani, I. Mirzaee, A. Shirvani and H. Shirvani, "An analytical approach for analysis and optimization of slider bearings with infinite width parallel textures," *Tribol. Int.*, vol. 43, pp. 1551–1565, 2010.
- [11] M. Fesanghary and M. Khonsari, "On the optimum groove shapes for load-carrying capacity enhancement in parallel flat surface bearings: theory and experiment," *Tribol. Int.*, vol. 67, pp. 254–262, 2013.
- [12] S. Malik and S.K. Kakoty, "Analysis of dimple textured parallel and inclined slider bearing," *Proc. Inst. Mech. Eng. Part J: J. Eng. Tribol.*, vol. 228, pp. 1343–1357, 2014.
- [13] L. Wang, W. Wang, H. Wang, T. Ma and Y. Hu, "Numerical analysis on the factors affecting the hydrodynamic performance for the parallel surfaces with microtextures," *J. Tribol.*, vol. 136, 021702-1–8, 2014.
- [14] J.H. Choo, H.A. Spikes, M. Ratoi, R. Glovnea and A. Forrest, "Friction reduction in low-load hydrodynamic lubrication with a hydrophobic surface," *Tribol. Int.*, vol. 40, pp. 154–159, 2007.
- [15] J.H. Choo, R.P. Glovnea, A.K. Forrest and H.A. Spikes, "A low friction bearing based on liquid slip at the wall," *ASME J. Tribol.*, vol. 129, pp. 611–620, 2007.
- [16] R.F. Salant and A.E. Fortier, "Numerical analysis of a slider bearing with a heterogeneous slip/no-slip surface," *Tribol. Trans.*, vol. 47, pp. 328–334, 2004.
- [17] T.V.V.L.N. Rao, "Analysis of single-textured slider and journal bearing with partial slip surface," *J. Tribol.*, vol. 132, 014501-1–014501-7, 2010.
- [18] T.V.V.L.N. Rao, A.M.A. Rani, T. Nagarajan and F.M. Hashim, "Analysis of slider and journal bearing using partially textured slip surface," *Tribol. Int.*, vol. 56, pp. 121–128, 2012.
- [19] M. Tauviqirrahman, R. Ismail, J. Jamari, D.J. Schipper, "Combined effect of texturing and boundary slippage in lubricated sliding contacts," *Tribol. Int.*, vol. 66, pp. 274–281, 2013.
- [20] R.F. Ausas, P. Ragot, J. Leiva, M. Jai, G. Bayada and G.C. Buscaglia, "The impact of the cavitation model in the analysis of microtextured lubricated journal bearings," *J. Tribol.*, vol. 129, pp. 868–875, 2007.
- [21] L. Wang, and C. Lu, "Numerical analysis of spiral oil wedge sleeve bearing including cavitation and wall slip effect," *Lubr. Sci.*, vol. 27(3), 193–207, 2015.
- [22] D. Gropper, L. Wang and T.J. Harvey, "Hydrodynamic lubrication of textured surfaces: A review of modeling techniques and key findings," *Tribol. Int.*, vol. 94, pp. 509–529, 2016.
- [23] A. Fatu, P. Maspeyrot and Hajjam, M, "Wall slip effects in (elasto) hydrodynamic journal bearings," *Tribol. Int.*, vol. 44, pp. 868–877, 2011.
- [24] M. Tauviqirrahman, Muchammad, R. Ismail, Jamari and D.J. Schipper, "Friction characteristics of liquid lubricated MEMS with deterministic boundary slippage," *J. Teknologi*, vol. 66 (3), pp. 75–80, 2014.
- [25] C.W. Wu, G.J. Ma and P. Zhou, "Low friction and high load support capacity of slider bearing with a mixed slip surface," *ASME J. Tribol.*, vol. 128, pp. 904–907, 2006.
- [26] F. Guo and P. L. Wong, "Theoretical prediction of hydrodynamic effect by tailored boundary slippage," *Proc. Ins. Mech. Eng. Part J: J. Eng. Tribol.*, vol. 220, pp. 43–48, 2006.
- [27] B. Jakobsson and L. Floberg, "The Finite journal bearing considering vaporization," *Chalmers Tekniska Hoegskola och Goteborgs Universitet, Geologiska Institutionen*, vol. 190, pp. 1–116, 1957.
- [28] K.O. Olsson, "Cavitation in dynamically loaded bearing," *Chalmers Tekniska Hoegskola och Goteborgs Universitet, Geologiska Institutionen*, vol. 308, pp. 1–60, 1965.
- [29] C.L.M.H. Navier, "Mémoire sur les lois du mouvement des fluides," *Mémoires de l'Académie Royale des Sciences de l'Institut de France* vol. 6, pp. 389–440, 1823.
- [30] A.R. Gherca, P. Maspeyrot, M. Hajjam and A. Fatu, "Influence of texture geometry on the hydrodynamic performances of parallel bearings," *Tribol. Trans.*, vol. 56, pp. 321–332, 2013.
- [31] S.V. Patankar, *Numerical heat transfer and fluid flow*, Levittown: Taylor & Francis; 1980.